



## A REVIEW OF METALLIC MATERIALS CORROSION

BY

OLGA POPA<sup>1,\*</sup>, ANA-MARIA ROȘU<sup>2</sup> and VALENTIN ZICHIL<sup>1</sup>

<sup>1</sup>“Vasile Alecsandri” University of Bacău, Faculty of Engineering,  
Department of Engineering and Management, Mechatronics

<sup>2</sup>“Vasile Alecsandri” University of Bacău, Faculty of Engineering,  
Department of Chemical and Food Engineering

Received: November 29, 2021

Accepted for publication: December 30, 2021

**Abstract.** The present manuscript presents a theoretical study for the corrosion process. Corrosion processes are primed and stimulated in 60% of cases by chemical and biological elements. One of the most used biological elements are: bacteria, actinomycetes, microscopic fungi, algae. Corrosion of a solid body results from the transformation of structural bonds in that body. Less than certain influences (water, oxygen, light, etc.) the atom - which is practically neutral - can lose or gain electrons and it is ionized.

Brake pads are affected of corrosion process. The conceptions and mathematical symbols serve as the models building blocks. Authors like, Boz M, and other authors demonstrate in their researches that starting with the concept of number, where every mathematical object is a mathematical model.

In practice it is not possible to reproduce some experimental, theoretical conditions related to corrosion processes. These processes are therefore, to some extent, different in terms of the applicability of theoretical laws. From a thermodynamic point of view, metals are not stable and due to corrosion, metals tend to return to the stable form of oxides with the help of oxygen and moisture in the air. For this each metal requires certain ionization energy.

---

\*Corresponding author; *e-mail*: [chirciu\\_olgutza@yahoo.com](mailto:chirciu_olgutza@yahoo.com)

© 2021 Olga Popa et al.

This is an open access article licensed under the Creative Commons Attribution-NonCommercial-NoDerivatives 4.0 International License (CC BY-NC-ND 4.0).

When establishing the mathematical model, those characteristics of the modeling object are highlighted, which, on the one hand, are informative, and on the other hand, they admit the mathematical form review.

**Keywords:** corrosion, mathematical model, atom, metallic materials.

## 1. Introduction

In most cases, the last result of corrosion reactions is weight variation. The corrosion rate may remain constant, rise, or decrease depending on the type of metal and the adverse environmental circumstances. The goal of this review is to gain a better understanding of the many wear mechanisms of material corrosion, as well as to improve their wear and properties. The primary wear modes in the graphite-free formed sample include abrasive and fragmental wear, as well as fatigue cracks, whereas the main wear mode in the graphite-containing substance is a glazed surface.

Cho M.H. and their collaborators show a considerable dispersion of graphite lubricant on the pad surface has been demonstrated after friction operations. As result, they demonstrate that a protective coating formed on the surface, lowering aggressive friction between the mating surfaces and enhancing adhesion forces between the hard particle and the composite mixture, which kept the hard particle inside. The first option is a brake pad material from Toyota Company that is employed as a material behaviour indicator in the industrial sector. The second material is an unaltered particle composite with no graphite lubricant. The third type is a modified brake pad, which contains a significant amount of modification ingredients (Cho *et al.*, 2006).

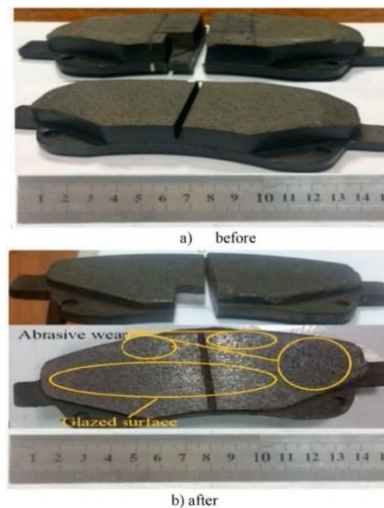


Fig. 1 – Examination of the genuine pad's surface (Nagwa, 2021).

Nagwa Ahmed Elzayady report the SEM microstructure and EDXS chemical composition are used to characterize the worn face's friction layers. An examination into charting has also been conducted. Also, EDXS analysis was used to identify some of the pad surface components prior to the service.

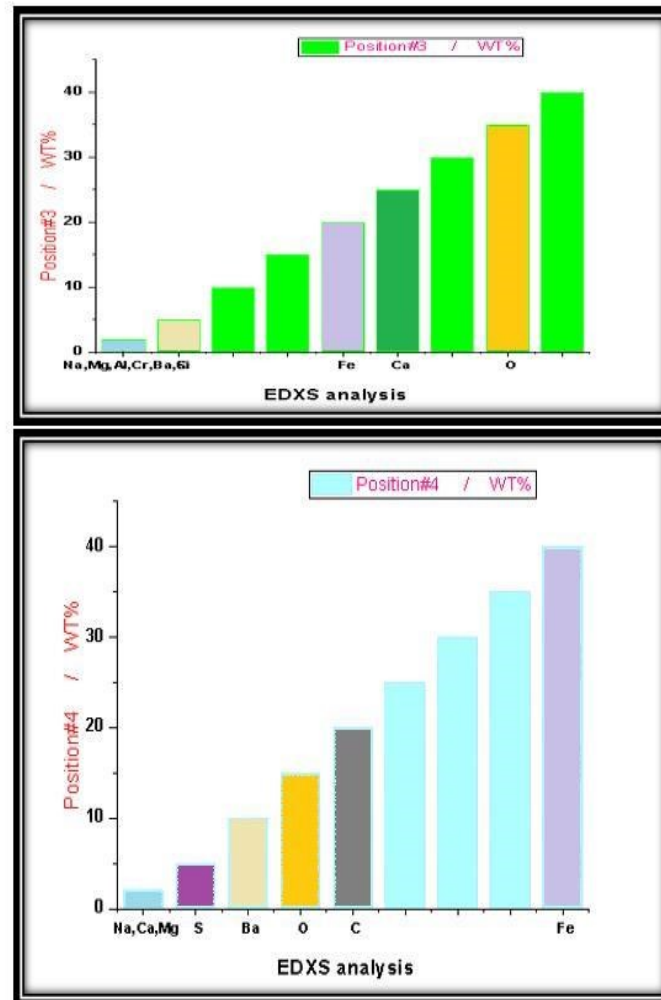


Fig. 2 – EDXS findings of the genuine pad were obtained prior to the service (Nagwa, 2021).

Chemical compositions at specific points on a complex material are not a trustworthy signal of the chemical evaluation of the entire surface, regardless of the results of the EDXS study. Authors as Usui E. and Nagwa A.E. report a list of investigation for the areal chemical were analysis has been advised to

learn more about the chemical behavior of the pad in such braking applications (Usui *et al.*, 1978).

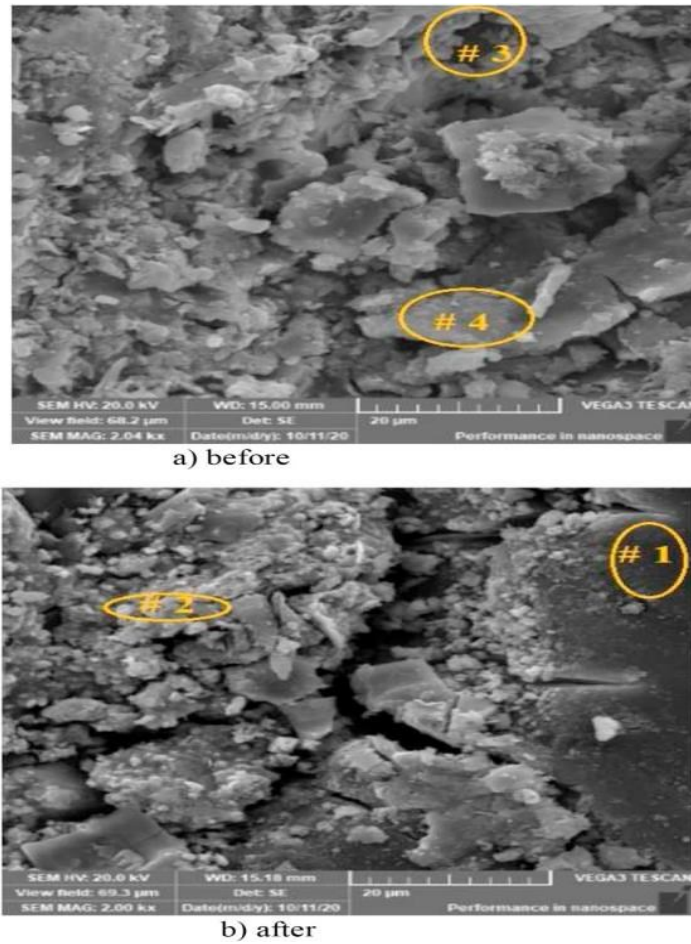


Fig. 3 – Before and after the service, SEM images of the genuine pad at 50 X magnification (Nagwa, 2021).

In mechanical processes, kinetic energy is transformed into potential energy and vice versa, their sum at any moment of time being constant.

$$\Delta E_c + \Delta E_p = 0 \text{ or } E = E_c + E_p = E_{c_0} + E_{p_0} = E_{c_{\max}} = E_{p_{\max}} = \max = \text{const.} \quad (1)$$

In fluid mechanics, the Navier-Stokes equation is a partial differential equation that describes the flow of incompressible fluids.

$$\frac{\partial u}{\partial t} + u \cdot \nabla u = -\frac{\nabla P}{\rho} \quad (2)$$

Where  $u$  is the fluid velocity vector,  $P$  is the fluid pressure,  $\rho$  is the fluid density, and  $\nabla$  indicates the gradient differential operator.

In contemporary notation, the Navier-Stokes equation is:

$$\frac{\partial u}{\partial t} + u \cdot \nabla u = -\frac{\nabla P}{\rho} + \nu \nabla^2 u \quad (3)$$

Where  $u$  is the fluid velocity vector,  $P$  is the fluid pressure,  $\rho$  is the fluid density,  $\nu$  is the kinematic viscosity, and  $\nabla^2$  is the Laplacian operator (see Laplace's equation).

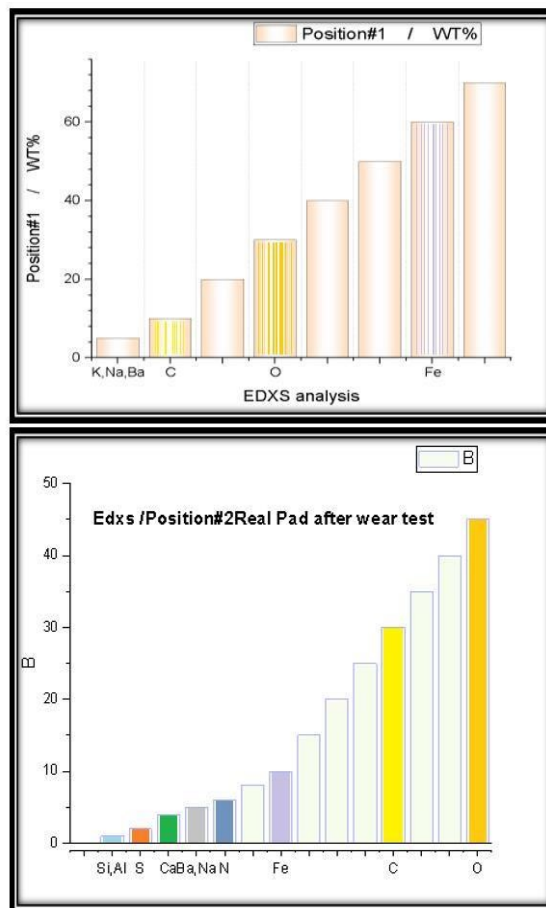


Fig. 4 – EDXS results of the real pad after wear testing (Nagwa, 2021).

Clarelli F. show that for a particle composite structure, the solution of the mapping shows the surface pad before service having a normal distribution. The components are agglomerated in some locations and decreased in others, resulting in an unequal concentration of elements in different regions. A specific element's distribution on the surface reflects the compound's distribution (Clarelli *et al.*, 2014).

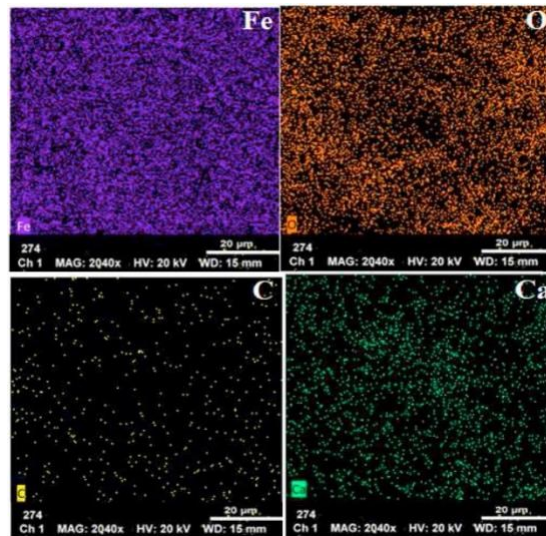


Fig. 5 – After service, mapping results of the real pad (Nagwa, 2021).

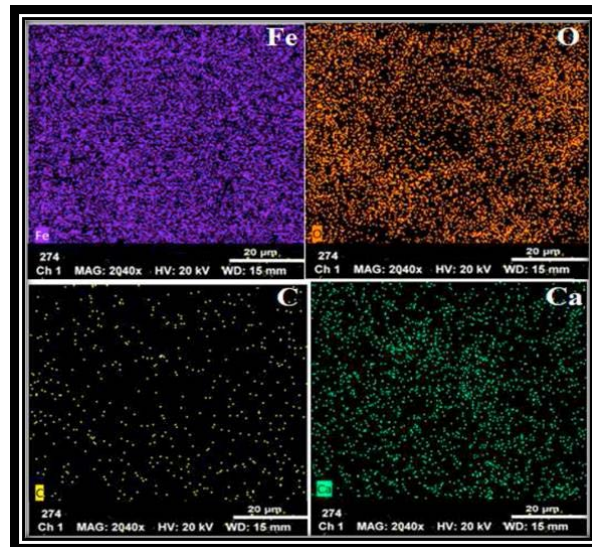


Fig. 6 – Before service, mapping the findings of the real pad, 2040 X (Nagwa, 2021).

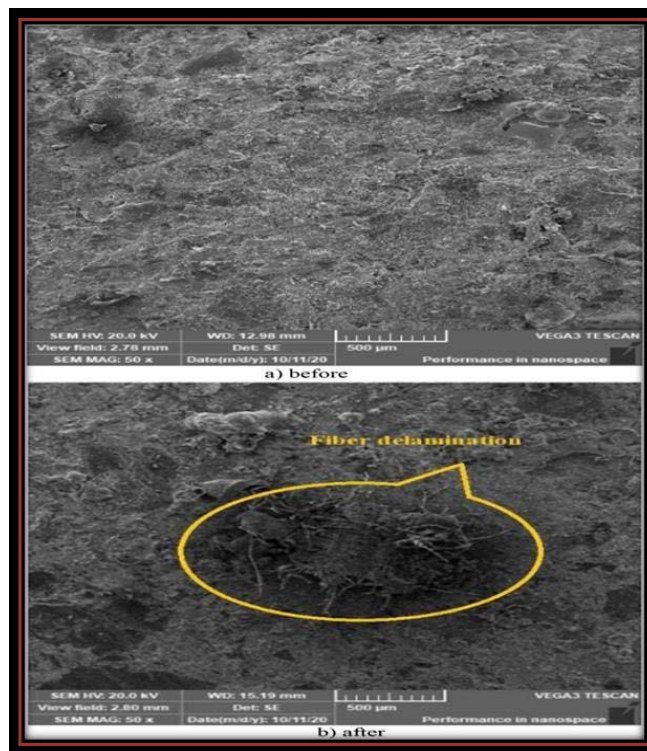


Fig. 7 – Before and after the service, SEM images of the genuine pad at 50 X magnification (Nagwa, 2021).

The allocation of a certain element reflects the distribution of its compound over the surface.

Figure 5 depicts this process for the elements Fe, O, C, Ca, Ba, Si, and S. However, following the real pad's lifetime, Fig. 6 shows a homogeneous distribution of the elements Fe, O, C, and Ca all over the surface, suggesting greater elemental diffusion over the surface via sliding motion. Figure 6 also shows a strong diffusion of Fe and O components (Nagwa, 2021).

This implies that after the life service, a substantial amount of iron oxides and carbon oxides are produced on the surface (Filip *et al.*, 2004).

The EDXS data from researches studies confirmed the fading of several phases (Filip *et al.*, 2004). Two fading phases that could exist are Si compounds and barium sulfate. Because of the contact pressure between the opposing surfaces, some of these phases may have been pyrolyzed, while others may have been abraded. On the faces of the formulated samples, SEM observations and EDXS analysis were performed. The authentic pad could not adequately compare the properties of the fabricated samples due to industrial and commercial issues. Grinding and fragmental wear, as well as fatigue cracks,

were the dominating wear modes in graphite-free produced samples (Li Xuewu *et al.*, 2019).

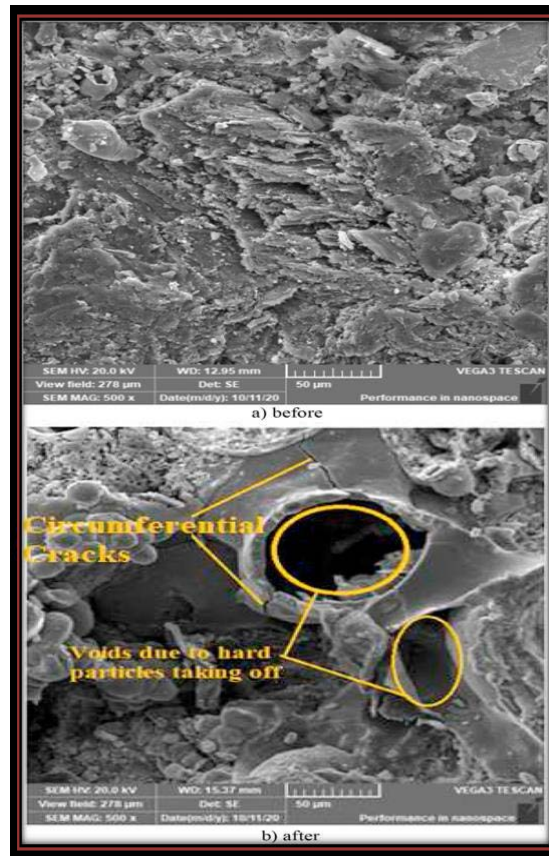


Fig. 8 – Images of SEM of the real pad at 500 X Magnification before and after the service (Nagwa, 2021).

When this sample is subjected to friction, the rough structure promotes hard particles to fly out, leaving big holes in the interior. Thermal fatigue, which happens as a result of the severe heat's wide temperature range, causes major cracks. The high diffusion of graphite lubricant emerges from friction sliding leads to the formation of a protective layer on the surface, which reduces surface roughness and so relieves the majority of surface-induced stresses.

Nagesh S.N. and collaborators demonstrate as result, that this layer boosts the material's strength by increasing the adhesion forces between the hard particles and the mixture and keeping them lodged inside. As a result, fragmental wear has greatly lowered (Nagesh *et al.*, 2014).

## 2. Mathematical modeling

Mathematical modeling has as general form the following scheme, described by Carelli F. and collaborators:

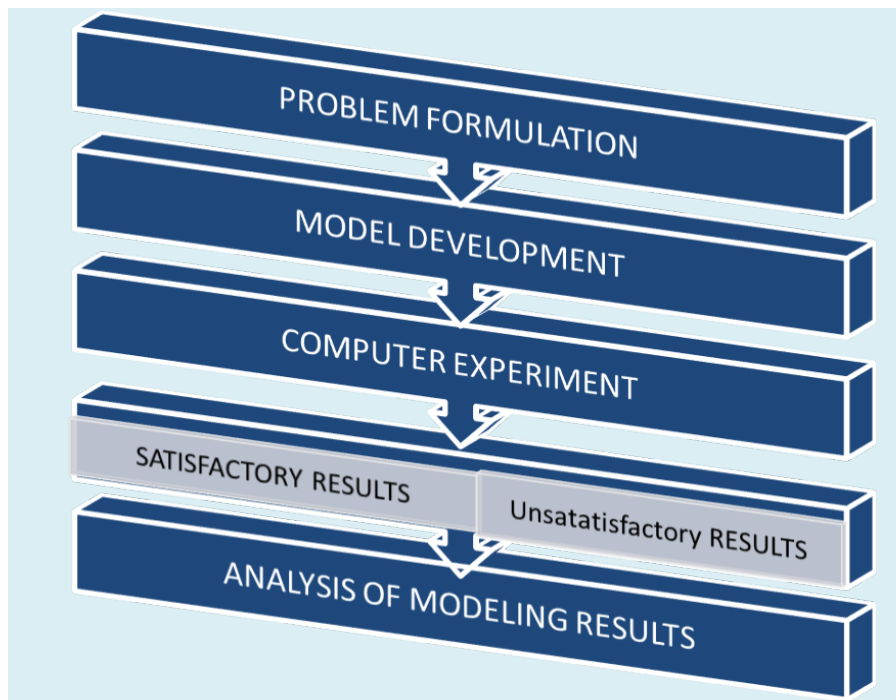


Fig. 9 – Scheme for mathematical model (Carelli *et al.*, 2000).

Thus, for the theoretical solution of a matter, it must be discretized in key points, which must be rigorously analyzed. Thus, formulation of the matter - represents the preparatory stage and involves the system that will have to be analyzed theoretically (Liew *et al.*, 2019).

Elaboration of the model:

- the stage involves the actual construction of the model;
- requires a very good knowledge of the system to be analyzed, as well as the theory to be applied, so a good understanding of reality and theory.

Computerized experiment - represents the analysis, in this case, with finite element a heat transfer in the case of the processing process mechanics (Carelli *et al.*, 2000). Analysis of the obtained results involves the comparison of the model theoretically analyzed with reality to validate or not initially conceived hypothesis.

It is observed that any mathematical model is based on a series of input variables and a series of output variables, which usually establishes the connection between the finished variables, their grouping being achieved by the causal orientation of the model (Perez *et al.*, 2019).

The classification of mathematical models according to the input and output variables can be done in the following form:

According to the character of the input-output relationship (Carelli *et al.*, 2000):

- models without memory - the output sizes at a given time depend only on the input sizes at the same time.

$$Y_{(t)} = X_{u_{(t)}} \quad (4)$$

- models with memory - models in which the output size depends essentially on the history of the previous evolution, in which case the mathematical representation is made by differential, integro-differential equations or partial derivatives.

- the transitional regime, in the case of these models, has a finite duration resulting in a variation, these models being also called dynamic models.

$$x = f_{(x_t, u_t)} \quad (5)$$

$$f_{(x_0, u_0)} = 0_{\text{stationary regime}} \quad (6)$$

By number of parameters:

- parametric models - models that, in order to be completely defined, require a finite number of parameters.

$$\rho_c \left( u \frac{\partial_T}{\partial_x} + v \frac{\partial_T}{\partial_y} \right) - \dot{q} = k \left( \frac{\partial^2_T}{\partial_{x^2}} + \frac{\partial^2_T}{\partial_{y^2}} \right) \quad (7)$$

- non-parametric models - in order to be completely characterized, these mathematical models demand an infinite number of parameters, these being infinitely dimensional a finite number of parameters.

By number of input-output variables

- monovariate models - a single input variable and a single output variable;

- multivariate models - have at least two input sizes and at least two output variables (Wang *et al.*, 2015).

According to the way of representing the variable sizes:

- variable sizes - continuous representation (take an infinity of values); - discrete representation (I take a finite number of values).

- mathematical models - continuous (quantities are continuous functions) and - discrete (sizes are discrete functions).

According to the character of the size variation:

- deterministic models - all variable sizes are deterministic;

- stochastic models - at least one size has a stochastic character

According to the character of the dependence of the variable sizes on the spatial coordinates:

- model with concentrated parameters - variable sizes of the model depend on a single variable with deterministic character (equations ordinary differentials);

- model with distributed parameters - at least one variable size depends of at least one spatial coordinate and of timing (partial derived equations).

The multitude of fields in which they can be used as well as the various forms of solving a problem, the mathematical models are classified in:

#### **Models**

- linear - mathematical interactions in which the variables have exponents equal to the unit;

- nonlinear - mathematical interactions in which variables with exponents intervene supraunitary;

- Deterministic and probabilistic models - used both for certain process as well as for processes with a high degree of uncertainty;

- Discrete and continuous models - used for mathematical completion a problems in which the phenomena have a distribution discrete or continuous distribution;

- Axiomatic models - the axiomatic system represents proportions expressed in form

Mathematics;

- Algorithmic models;

- Smart models;

- Stationary models.

Brief introduction in the act of the doctoral topic the doctoral topic has as main purpose the analysis of the effects produced by external agencies on the quality of metal sheets used in industry. Corrosion may be defined as a gradual deterioration of the metallic material by chemical reactions with the environment. Corrosion of metal tables is a very complex process, which can be explained by multiple methods as a potential theory, respectively electrochemical (Rhee *et al.*, 1991).

It can be found in anodic environments/niches that can be detailed according to the reaction below:



Where:  $n = 1, 2, 3, 4$

All electrons generated by anodic reactions are described by Carelli F and collaborators as:

1. Reduction of hydrogen ions:



2. The oxygen reduction (in acid solution):



3. The oxygen reduction (in basic or neutral solution):



4. Metal ion reduction:



where  $n = 1, 2, 3, \dots$

The corrosion rate is calculated according to the description of Carelli F. and collaborators in their researches as:

$$(\text{mg} \cdot \text{cm}^{-2} \cdot \text{s}^{-1}) = \frac{W}{A \times t} \quad (13)$$

where:  $W$  – total mass during the corrosion process;  $A$  – surface exposed to corrosion;  $t$  – time of acting.

Example of mathematical model for calculating the corrosion rate for the corrosion process is in the case of metal sheets containing Copper (Carelli *et al.*, 2000).

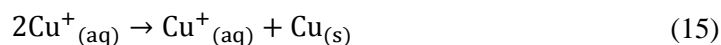
The complexity of the corrosion process requires quantitative models to simulate and understand the processes developed as a solution of this action. Mathematical models are helpful in simulating, monitoring and detecting alternate surfaces before they become visible. These mathematical models make it possible to determine the optimal strategies on the process.

For example of a mathematical model, was chosen an existing copper corrosion model in 904 L type stainless steels in which the Cu content is 13.4%.

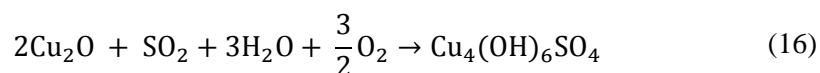
The characteristic chemical reaction is:



When the Cu-containing metal sheet is exposed to moisture or sulfur dioxide ( $\text{SO}_2$ ) in the atmosphere, three types of Cu mineral salt can be produced, the most important of which is  $\text{Cu}_4\text{SO}_4(\text{OH})_6$ , called brochantite or sulfate Cu mineral. The variation of the pH leading to the formation of Cu ions which by oxidation give cupric ions:



The mathematical model was used and applied and involves primarily detailing the chemical reaction that occurs (Boz M. *et al.*, Cho M.H.):



Simulation involves scoring with:

$\alpha(t)$  – the layer between Cu and cuprite;  $\beta(t)$  – the layer between copper and brochantite;  $\gamma(t)$  – the layer between brochantite and the external environment

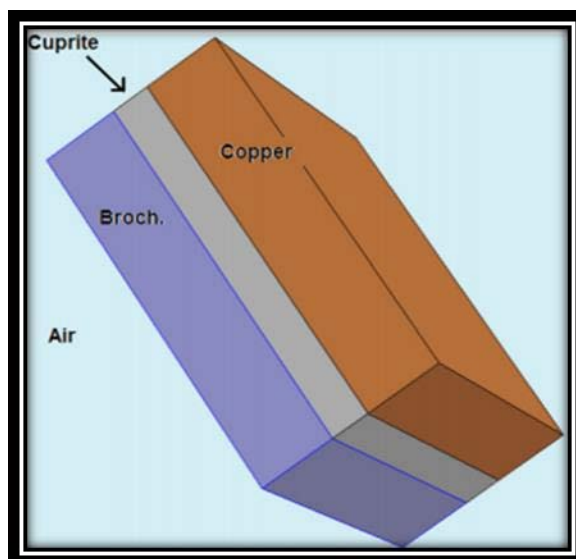


Fig. 10 – Example of layers (Carelli *et al.*, 2000).

The reaction time  $S_1$  is:

$$\dot{S}_1 = -\omega_\rho \dot{\alpha} \quad (17)$$

Where

$$\omega_\rho = \frac{\mu_c}{2\mu_\rho} - 1 \quad (18)$$

Where:  $\mu_c$  and  $\mu_\rho$  = molar density (moles/cm<sup>3</sup>) of Cu and Cu<sub>2</sub>O  
In case of

$$\omega_\rho > 0 \quad (19)$$

→  $\mu_c$  and  $\mu_\rho$  = constants →

$$S_1(t) = -\omega_\rho \alpha(t) \quad (20)$$

The physical boundary between cuprite and brochantite is given by:

$$\beta(t) = b(t) + S_1(t) \quad (21)$$

Where:  $b(t)$  = copper consumption obtained by the equation:

$$\dot{S}_2(t) = -\omega_b \dot{b}(t) \quad (22)$$

Where

$$\omega_b = \frac{\mu_\rho}{2\mu_b} - 1 \quad (23)$$

$\mu_\rho$  = molar density (moles/cm<sup>3</sup>) of flea market

The variation with the external environment being given by:

$$\dot{\gamma} = -\omega_\rho \dot{\alpha}(t) - \omega_b \dot{b}(t) \quad (24)$$

The area of brochantitis formation is given by

$$\gamma(t) \leq x \leq \beta(t) \quad (25)$$

and the Cu oxide area is given by

$$\beta(t) \leq x \leq \alpha(t) \quad (26)$$

The flow of sulfur dioxide in the environment relative to the air is given by Fick's law. Thus, the SO<sub>2</sub> flux is given by the equation:

$$J_s = n_b \left( -D_s \frac{\partial S}{\partial X} - S\omega_\rho \dot{\alpha} - S\omega_b \dot{b} \right) = n_b \left( -D_s \frac{\partial S}{\partial X} + S\dot{\gamma} \right) \quad (27)$$

Where:

- the first term refers to the diffusion of SO<sub>2</sub> in the brochantite layer;
- nb = porosity of the brochantite layer;
- D<sub>s</sub> = diffusibility;
- Sω<sub>ρ</sub>α̇ and –Sω<sub>b</sub>ḃ are terms that refer to swelling caused by the formation of copper and brochantite.

Therefore, the mass of SO<sub>2</sub> in the brochantite layer

$$\gamma(t) \leq x \leq \beta(t) \quad (28)$$

is determined by the equation:

$$\frac{\partial S}{\partial t} - D_s \frac{\partial^2 S}{\partial X^2} + \dot{\gamma} \frac{\partial S}{\partial X} = 0 \quad (29)$$

The value S at the external limit γ (t) is the concentration of the medium in SO<sub>2</sub>, which can be found as a function of time according to the equation:

$$S(\gamma(t)) = S_a(t) \quad (30)$$

If the molar flux of SO<sub>2</sub> at the limit of β (t) is proportional to the consumption of Cu<sub>2</sub>O moles, then it's necessary to follow the equation:

$$-n_b \frac{D_s}{M_s} \frac{\partial S}{\partial X} = \frac{1}{2} \frac{\rho_p}{M_p} \dot{b} \quad (31)$$

Where:

- M<sub>s</sub>, M<sub>p</sub> represents the molecular mass of SO<sub>2</sub>, respectively Cu<sub>2</sub>O;
- ρ<sub>p</sub> represents the density of copper (Su *et al.*, 2015).

Similarly in the case of moisture flow result:

$$J_w = n_b \left( -D_w \frac{\partial W}{\partial X} - W\omega_\rho \dot{\alpha} - W\omega_b \dot{b} \right) = n_b \left( -D_w \frac{\partial W}{\partial X} + W\dot{\gamma} \right) \quad (32)$$

Where:  $D_w$  – water diffusibility

Thus, the material balance in the brochantite layer is represented by the equation:

$$\frac{\partial W}{\partial t} - D_w \frac{\partial^2 W}{\partial X^2} + \dot{\gamma} \frac{\partial W}{\partial X} = 0 \quad (33)$$

The value of  $W$  at the external limit  $\gamma(t)$ , is the concentration in experiments of water  $W_a(t)$ :

$$W(\gamma(t)) = W_a(t) \quad (34)$$

Since, the numbers of moles of water are consumed in the chemical equation; at the limit  $\beta(t)$  it's necessary to follow the mathematical equation:

$$\frac{J_w}{M_w} = \frac{3 \rho_p}{2 M_p} \dot{b} + n_b \frac{W}{M_w} \dot{b} \quad (35)$$

Finally, the oxygen flow is given by the equation:

$$J_o = n_b \left( -D_o \frac{\partial O}{\partial X} + O \dot{\gamma} \right) \quad (36)$$

Where:  $D_o$  – oxygen diffusibility.

The material balance of the brochantite layer being given by the equation:

$$\frac{\partial O}{\partial t} - D_o \frac{\partial^2 O}{\partial X^2} + \dot{\gamma} \frac{\partial O}{\partial X} = 0 \quad (37)$$

Copper layer-specific equations involve chemical reactions between oxygen and copper. Oxygen flux can be calculated using the equation:

$$J_g = n_p \left( -D_g \frac{\partial G}{\partial X} - G \omega_p \dot{\alpha} \right) \quad (38)$$

The equation specifies the material balance being:

$$\frac{\partial G}{\partial t} - D_g \frac{\partial^2 G}{\partial X^2} - \omega_p \dot{\alpha} \frac{\partial G}{\partial X} = 0 \quad (39)$$

The value of  $G_p$ , at the limit  $\beta(t)$  is given by the value of oxygen obtained from the equation:

$$\frac{J_o}{M_o} = \frac{3 \rho_p}{4 M_p} \dot{b} + n_b \frac{O}{M_o} \dot{b} \quad (40)$$

The solutions of the mathematical model describe and simulate the evolution of the formation of the brochantite layer in the exposure of the metal sheets with a high copper content, in the sulphurous dioxide atmosphere. From the laboratory, this model may be controlled and applied after authors as Su L. and collaborators (Su *et al.*, 2015).

### 3. Conclusions

As a conclusion of the current review analysis, the different wear modes in the real pad have been identified as:

a) abrasion damage manifested as a glazed surface with a deep depth, abrasive wear, and eroded phases;

b) thermo-mechanical (fatigue) wear, manifested as massive broken surfaces as a result of thermal fatigue;

c) physical deterioration due to the production of rust layers and, as a result, corroded surfaces, as evidenced by the dense diffusion of iron, oxygen, and carbon molecules;

d) thermo-chemical wear (phases pyrolysis - These types of wear are rarely prevented in real-world operation, but they can be reduced by minimizing excessive heat in the brake, avoiding excessive use, poor break-in of new pads, and selecting proper material ingredients that reduce excessive heat.

When friction is applied to this sample's rigid structure, the hard particles fly out, leaving big holes inside. Thermal fatigue, which is produced by the broad temperature range induced by the severe heat, also causes major cracks. Adding graphite to the friction material, on the other hand, minimizes the heat generated during friction between the brake pad and the bearing surface, resulting in less excessive heat at the brake pad's exterior. The high diffusion of graphite lubricant emerges from friction sliding leads to the formation of a protective layer on the surface, which reduces surface roughness and so relieves the majority of surface-induced stresses. This layer improves the material's strength by boosting the adhesion forces between the hard particles and the mixture, allowing them to stay lodged inside. The amount of fragmental wear has been drastically reduced (Verma *et al.*, 2015).

## REFERENCES

- Aslama R., Serdaroglu G., Zehraa S., Vermac D.K., Aslamd J., Guoe L., Vermaf C., Eno E E., Quraishif M.A., *Corrosion inhibition of steel using different families of organic compounds: Past and present progress*, Journal of Molecular Liquids, Vol. **348**, 15 February 2022, 118373 (2022).
- Azmi N.S.M., Mohamed D., Tadza M.Y.M., *Effects of various relative humidity conditions on copper corrosion behavior in bentonite*, Materials Today: Proceedings, Vol. **48**, Part 4, 2022, 801-806 (2022).
- Boz M., Kurt A., *Effect of ZrSiO<sub>4</sub> on the friction performance of automotive brake friction materials*, J Mater Sci Technol, **23**, 6 (2007).
- Canakcı A., Ozkaya S., Erdemir F., Kabacak A.H., Celebi M., *Effects of Fe–Al intermetallic compounds on the wear and corrosion performances of AA2024/316L SS metal/metal composites*, Journal of Alloys and Compounds, Vol. **845**, 156236 (2020).
- Chen J., Zhao Y., Gao H., Chen S., Li W., Liu X., Hu X., Yan S., *Rolled electrodeposited copper foil with modified surface morphology as anode current collector for high corrosion resistance in lithium-ion battery electrolyte*, Surface and Coatings Technology, Vol. **421**, 127369 (2021).
- Cho M.H., Kim S.J., Kim D., Jang H., *Effects of ingredients on tribological characteristics of a brake lining: an experimental case study*, Wear 2006, 258:1682.
- Clarelli F., De Filippo B., Ntalini R., *Mathematical model of copper corrosion*, Applied Mathematical Modelling, 38, 4804-4816 (2000).
- El-Hossainy T.M., El-Shazly M.H., Abd-Rabou M., *Finite element simulation of metal cutting considering chip behavior and temperature distribution*, Mater. Manuf. Process., **16**, 6, 803-814 (2001).
- Filip P., Weiss Z., Rafaja D., *On friction layer formation*, 2002.
- Guo X., Vullum P.E., Venvik H.J., *Inhibition of metal dusting corrosion on Fe-based alloy by combined near surface severe plastic deformation (NS-SPD) and thermochemical treatment*, Corrosion Science, Vol. **190**, 109702 (2021).
- Jiang M., Gao Y., Patil S.A., Hou H., Feng W., Chen S., *Reactive coating modification of metal material with strong bonding strength and enhanced corrosion resistance for high-performance bioelectrode of microbial electrochemical technologies*, Journal of Power Sources, Vol. **491**, 229595 (2021).
- Jun J., Tortorelli P.F., 4.18 - *Corrosion in Other Liquid Metals (Li, PbLi, Hg, Sn, Ga)*, Editor(s): Rudy J.M. Konings, Roger E. Stoller, Comprehensive Nuclear Materials (Second Edition), Elsevier, 515-527 (2020).
- Li X., Shi T., Li B., Chen X., Zhang C., Guo Z., Zhang Q., *Subtractive manufacturing of stable hierarchical micro-nano structures on AA5052 sheet* (2019).
- Liew K.W., Nirmal U., *Frictional performance evaluation of newly designed brake pad materials*, Mater, 2013.
- Lin X., Han E.-H., Peng Q., Ke W., Jiao Z., *Effect of postirradiation annealing on microstructure and corrosion of proton-irradiated 308L stainless steel weld metal*, Corrosion Science, Vol. **175**, 108887 (2020).

- Liu R., Liu L., Wang F., *The role of hydrostatic pressure on the metal corrosion in simulated deep-sea environments - a review*, Journal of Materials Science & Technology, Vol. **112**, 230-238 (2022).
- Liu Z., Ye Y.W., Chen H., *Corrosion inhibition behavior and mechanism of N-doped carbon dots for metal in acid environment*, Journal of Cleaner Production, Vol. **270**, 122458 (2020).
- Mingear J., Hartl D., *Liquid metal-induced corrosion of nickel-titanium alloys by gallium alloys for liquid metal-enabled shape memory applications*, Corrosion Science, Vol. **167**, 108524 (2020).
- Nagesh S.N., Siddaraju C., Prakash S.V., Ramesh M.R., *Characterization of brake pads by variation in composition of friction materials*, Proc Mater Sci, 2014, 5:295e302.
- Osterle W., Prietzel C., Dmitriev A.I., *Investigation of surface film nanostructure and assessment of its impact on friction force stabilization during automotive braking*, Int J Mater Res (2010).
- Perez B., Echeberria J., *Influence of abrasives and graphite on processing and properties of sintered metallic friction materials*, Heliyon (2019).
- Priya R., Thyagarajan K., Thinaharan C., Vijayalakshmi S., Ningshen S., *Role of noble metal fission products on the microstructural evolution and corrosion behaviour of ferritic steel-Zr based metal waste form alloys in the simulated repository environment*, Journal of Alloys and Compounds, Vol. **820**, 153168 (2020).
- Rhee S.K., Jacko M.G., Tsang P.H.S., *The role of friction film in friction, wear and noise of automotive brakes*, 1991.
- Shalabi K., Abdel-Galil E., El-Askalany A.H., Abdallah Y.M., *Adsorption, Electrochemical Behavior, and Theoretical Studies for Copper Corrosion Inhibition in 1 M Nitric acid Medium using Triazine Derivatives*, Journal of Molecular Liquids, Vol. **348**, 118420 (2022).
- Shen J., Yang D., Ma L., Gao Z., Yan A., Liao Q., *Exploration of neonicotinoids as novel corrosion inhibitors for copper in a NaCl solution: Experimental and theoretical studies*, Colloids and Surfaces A: Physicochemical and Engineering Aspects, Vol. **636**, 128058 (2022).
- Silva E.F., Wysard J.S., Bandeira M.C.E., Mattos O.R., *Electrochemical and surface enhanced Raman spectroscopy study of Guanine as corrosion inhibitor for copper*, Corrosion Science, Vol. **191**, 109714 (2021).
- Su L., Gao F., Han X., Fu R., Zhang E.M., *Tribological behavior of copper-graphite powder third body on copper-based friction materials*, Tribol Lett 2015; 60(2):1.
- Tokita S., Kadoi K., So A., Inoue H., *Relationship between the microstructure and local corrosion properties of weld metal in austenitic stainless steels*, Corrosion Science, Vol. **175**, 108867 (2020).
- Usui E., Shirakashi T., Kitagawa T., *Analytical prediction of three dimensional cutting process, Part 3: Cutting temperature and crater wear of carbide tool*, Transactions of ASME, Journal of Engineering for Industry 100 (1978) 236-243.
- Verma P.C., Menapace L., Bonfanti A., Ciudin R., Gialanella S., Straffelini G., *Braking pad-disc system: wear mechanisms and formation of wear fragments*, 2015.
- Wang R., Farid M.M., *Corrosion and health aspects in ohmic cooking of beef meat patties*, Journal of Food Engineering, **146**, 17-22 (2015).

- Xia D.-H., Deng C.-M., Macdonald D., Jamali S., Mills D., Luo J.-L., Strebl M.G., Amiri M., Jin W., Song S., Hu W., *Electrochemical measurements used for assessment of corrosion and protection of metallic materials in the field: A critical review*, Journal of Materials Science & Technology, Vol. 112, 151-183 (2022).
- Zhang X., Li S., Sun W., Wang L., Wang J., Liu G., *Study on the corrosion behavior of copper coupled with TiO<sub>2</sub> with different crystal structures*, Corrosion Science, Vol. 183, 109352 (2021).
- Zhao W., Babu R.P., Chang T., Odnevall I., Hedström P., Johnson C.M., Leygraf C., *Initial atmospheric corrosion studies of copper from macroscale to nanoscale in a simulated indoor atmospheric environment*, Corrosion Science, Vol. 195, 109995 (2022).
- Zhao W., Chang T., Leygraf C., Johnson C.M., *Corrosion inhibition of copper with octadecylphosphonic acid (ODPA) in a simulated indoor atmospheric environment*, Corrosion Science, Vol. 192, 109777 (2021).
- Zou C., Zhou Q., Wang X., Zhang H., Wang F., *Cationic polyurethane from CO<sub>2</sub>-polyol as an effective barrier binder for polyaniline-based metal anti-corrosion materials*, Electronic supplementary information (ESI) available: Synthesis details, spectroscopic characterization, etc. See DOI: 10.1039/d0py01757d, Polymer Chemistry, Vol. 12, Issue 13, 1950-1956 (2021).

## O ANALIZĂ A COROZIUNII MATERIALELOR METALICE

(Rezumat)

Lucrarea de față prezintă un studiu teoretic pentru procesul de coroziune. Procesele de coroziune sunt inițiate și stimulate în 60% dintre cazuri de elemente chimice și biologice. Unele dintre cele mai utilizate elemente biologice sunt: bacteriile, actinomicetele, ciupercile microscopice, algele. Coroziunea unui corp solid rezultă din transformarea legăturilor structurale din acel corp. Mai puțin de anumite influențe (apă, oxigen, lumină etc.) atomul - care este practic neutru - poate ceda sau căpăta electroni și este ionizat.

Plăcuțele de frână sunt afectate de procesul de coroziune. Concepțiile și simbolurile matematice servesc ca elemente de construcție ale modelelor. Autori ca, Boz M, și alți autori demonstrează în cercetările lor că pornind de la conceptul de număr, unde fiecare obiect matematic este un model matematic.

În practică nu este posibilă reproducerea unor condiții experimentale, a unor condiții teoretice legate de procesele de coroziune. De aceea, aceste procese sunt, într-o oarecare proporție, diferite în ceea ce privește aplicabilitatea legilor teoretice. Din punct de vedere termodinamic, metalele nu sunt stabile și, din cauza fenomenului de coroziune, metalele tind să revină la forma stabilă de oxizi cu ajutorul oxigenului și al umidității din aer. Pentru aceasta, fiecare metal are nevoie de o anumită energie de ionizare.

La stabilirea modelului matematic sunt evidențiate acele caracteristici ale obiectului de modelare, care, pe de o parte, sunt informative, iar pe de altă parte, admit analiza formei matematice.